

# Axon fasciculation and differences in midline kinetics between pioneer and follower axons within commissural fascicles

Magdalena Bak and Scott E. Fraser\*

Division of Biology, Biological Imaging Center, Beckman Institute, California Institute of Technology, Pasadena, CA 91125, USA

\*Author for correspondence (e-mail: sefraser@caltech.edu)

Accepted 1 July 2003

Development 130, 4999-5008  
© 2003 The Company of Biologists Ltd  
doi:10.1242/dev.00713

## Summary

**Early neuronal scaffold development studies suggest that initial neurons and their axons serve as guides for later neurons and their processes. Although this arrangement might aid axon navigation, the specific consequence(s) of such interactions are unknown in vivo. We follow forebrain commissure formation in living zebrafish embryos using timelapse fluorescence microscopy to examine quantitatively commissural axon kinetics at the midline: a place where axon interactions might be important. Although it is commonly accepted that commissural axons slow down at the midline, our data show this is only true for leader axons. Follower axons do not show this behavior. However, when the leading axon is ablated, follower axons**

**change their midline kinetics and behave as leaders. Similarly, contralateral leader axons change their midline kinetics when they grow along the opposite leading axon across the midline. These data suggest a simple model where the level of growth cone exposure to midline cues and presence of other axons as a substrate shape the midline kinetics of commissural axons.**

Movies available online

Key words: Forebrain, Zebrafish, Commissural axon, Neuronal scaffold, Growth cone, Intermediate target, Growth cone morphology, Growth cone behavior, GATA2, Axon pathway

## Introduction

During development of the central nervous system (CNS), neurons differentiate and connect with one other, enabling information processing and the establishment of specific behavioral patterns. A better understanding of the early events in neuronal connectivity in the forebrain is a fundamental step in understanding how the brain assembles itself and functions. Unlike their adult counterparts, early embryonic brains are relatively simple, with a small number of neurons and neuronal tracks, offering unique advantages for mechanistic studies. Detailed studies of tract formation in invertebrate nervous systems have shown that a small number of early neurons, termed pioneers, lay down an axonal scaffold that later axons and their growth cones follow (Bate, 1976; Bentley and Keshishian, 1982; Bastiani et al., 1984; Jacobs and Goodman, 1989; Boyan et al., 1995). Removal of these pioneers adversely affects the pathfinding of later axons (Raper et al., 1984; Klose and Bentley, 1989; Gan and Macagno, 1995; Hildalgo and Brand, 1997). Growth cones of pioneer and later axons differ in their morphology: early axons possess larger and more complex growth cones (LoPresti et al., 1973; Bastiani et al., 1984). And growth cone morphology changes correlate with specific choice points along the axon route (Myers and Bastiani, 1993).

Analogous mechanisms may be involved in establishing the initial neuronal circuitry in vertebrates. For example, connections between the cerebral cortex and the thalamus originate from a transient population of subplate neurons that establish this connection during embryonic stages (McConnell et al., 1989). Using fluorescent lipophilic dye tracers, growth cone morphology differences between these early axons and

later axons found in this projection, have been observed in ferrets and cats (Kim et al., 1991). Growth cone morphology has been correlated with axon decision making, especially at choice points such as the optic chiasm and the floor plate. In these regions, growth cone morphology and sometimes growth behavior significantly change, with pioneering growth cones assuming complex shapes while later axons have more streamline growth cones (Bovolenta and Dodd, 1990; Wilson and Easter, 1991; Mason and Wang, 1997). Similar to invertebrate systems, the earliest axons in vertebrates are in the right place and at the right time to establish initial projections that later axons can then follow. For example, in zebrafish, secondary motoneurons in the absence of primary motoneurons are not able to correctly pattern dorsal nerves but do form correct, albeit delayed, ventral projections (Pike et al., 1992). Taken together, these data support the hypothesis that initial axons might play a pioneer-like role in establishing later axonal tracts, perhaps similar to their role in invertebrates. In vivo time-lapse analysis of axonal tract formation is needed to directly address how the initial axons affect later axons during early neuronal scaffold formation.

At one day of development, the zebrafish forebrain neuronal scaffold contains several distinct bilaterally symmetrical clusters of neurons, interconnected by a limited number of neuronal tracts and commissures (Chitnis and Kuwada, 1990; Wilson et al., 1990; Ross et al., 1992) (Fig. 1B), analogous to the early neuronal scaffold of mouse embryos (Mastick and Easter, 1996). During the next few days, the scaffold increases in size as more neurons and axons are added to the existing tracts, but few new axonal tracts appear. For example, initially the postoptic commissure (POC) connects two clusters of

ventral neurons (the left and right ventrorostral cluster; vrc) in the forebrain (Ross et al., 1992) (Fig. 1B) with additional axons from other brain regions projecting across it at later stages (Wilson and Easter, 1991). In zebrafish, cell labeling methods in combination with surgical manipulations reveal that early brain tracts aid in axon guidance for initial axons of other tracts (Chitnis and Kuwada, 1991; Wilson and Easter, 1991; Chitnis et al., 1992). Whether early axons influence later axons inside the same axon fascicles has not been addressed.

Here we build upon studies of the retinotectal projection (Hutson and Chien, 2002), olfactory neuron pathfinding (Dynes and Ngai, 1998), and growth cone and dendrite dynamics of spinal cord motoneurons (Jontes et al., 1999) to examine the role of early axon guides on midline kinetics of commissural axons. Using a stable transgenic zebrafish line (Meng et al., 1997) and timelapse confocal laser-scanning microscopy we reveal a new level of complexity in commissural axon kinetics at the midline. Our data shows that midline kinetics in vertebrate commissural axons result from the combination of highly adaptive axons, dynamics interaction between them and the different exposure of each growth cone to other axons and the local cues.

## Materials and methods

### Fish maintenance

Raising and spawning of adult zebrafish were performed as outlined in the Zebrafish book (Westerfield, 1995) and in accordance with the guidelines of the California Institute of Technology.

### Whole-mount immunohistochemistry and confocal microscopy

Embryos at stages 19–27 hpf were fixed, blocked and incubated with primary antibodies as previously described (Wilson et al., 1990). Acetylated alpha tubulin antibody (Sigma) was used to label neuronal cell bodies and their axons (Wilson et al., 1990; Ross et al., 1992). For some experiments, a cocktail of neuron specific antibodies zn1,8,12 (Developmental Studies Hybridoma Bank) was used for neuronal cell body labeling. The neuron specific antibodies were detected with secondary TRITC antibody (Jackson Lab). Inherent GFP was imaged. Embryos were deyolked prior to imaging and the head region (anterior to hindbrain) was dissected for imaging. Embryo heads were placed in bridge slides, covered with coverslips and imaged using the Zeiss LSM510 laser-scanning confocal microscope at 40 $\times$ .

### Timelapse confocal microscopy

Embryos at 20–22 hpf were anesthetized with tricaine in sedative amounts (0.01%) and embedded in a drop of 1–1.2% ultralow melt agarose on a cover slip-bottom petri dish in 30% danieau/0.01%tricaine/0.15 mM PTU (to bleach pigment). Imaging was performed using inverted Zeiss Pascal confocal with a Plan-Neuofluar 40X/N.A1.3 oil objective as well as Zeiss 510 confocal with Achroplan IR 40 $\times$ /0.8 W, 63 $\times$ /0.9W and C-Apochromat 40 $\times$ /N.A 1.2 objectives. Three-dimensional stacks of the forebrain were taken at 6, 3 and 1.5 minute intervals spanning the vrc and the POC. Temperature was maintained at 28–29 $^{\circ}$ C throughout all imaging. GFP-positive cells were excited with the 488 nm argon laser line using 505LP chroma filter set. Typical imaging experiment ( $n=22$  separate live specimens) lasted between 3–5 hours. A  $z$ -stack spanning approximately 60  $\mu$ m was collected at each time point with individual sections being 1  $\mu$ m apart. The pinhole settings were at 2.0–2.77 airy units. Refocusing was minimal but needed to be done occasionally to make sure the growth cones were imaged in full.  $z$ -stack images were

imported into Object Image and maximum intensity projections (MIPs) were made at each time point. These were later assembled into movies.

### Axon growth rates analysis

Time-lapse data were analyzed with a 4D visualization software (Slidebook Intelligent Imaging Innovations), which allowed us to import our movies from Object Image and trace individual axon lengths at each time point during the time-lapse. Midline was found using a transmitted light image from each timelapse. Axons were traced, measured and plotted as variation in position (distance) from midline along the arc of the POC trajectory (Fig. 3G). Axon lengths were also used to compute average growth rates. All axon length data were divided into two groups: axons with no commissure [i.e. leading axons ( $n=16$ )] and those where a commissure was already in place [i.e. follower axons ( $n=24$ )]. For each axon, the average growth rate $\pm$ s.e.m at midline, defined as  $\pm 10 \mu$ m on each side of the midline was calculated. The growth rate was compared to the average growth rate $\pm$ s.e.m. outside the midline for both axon groups. To confirm that our sampling time interval was adequate, timelapses were carried out at 1.5, 3 and 6 minute intervals and the numbers were analyzed separately for each group. Because all data were consistent across the different sampling frequencies, they were pulled together for final analysis.

### Dil labeling

Gata::GFP embryos were prepared for timelapse experiment and imaged until the first GFP-expressing growth cone appeared. The embryos were removed and immediately fixed in 4% PFA for 1.5 hours at room temperature. Fixed embryos were remounted in 1% agarose in PBS and injected under fluorescent microscope with DiI into the GFP-positive vrc cluster in order to label axons from the vrc cells. DiI-injected embryos were incubated at room temperature for 12–24 hours to allow the dye to diffuse throughout the axons and growth cones. Embryos heads were removed and remounted in agarose for analysis. Imaging was carried out using Zeiss Pascal inverted confocal scanning microscope, using 488 nm and 543 nm excitation sequentially using multitrack mode and a C-Apochromat 40 $\times$ /1.2 water objective.

### Growth cone morphology analysis

The highest quality time-lapses were selected for this analysis. Growth cone morphology was analyzed using ImageJ measurement and analysis software. Growth cone areas were measured by outlining the growth cone excluding filopodia. For width/length ratio measurements, the lengths of the growth cones were measured from tip of the leading edge of the lamellipodium to the base of the growth cone tip along a trajectory of the proximal region of that growth cone's axon. The width was measured in each case as the perpendicular segment positioned at the widest point for each growth cone. The average growth cone area $\pm$ s.e.m. and w/l ratio value were calculated and compared between leading and follower growth cones. The number and lengths of filopodia were recorded for each time frame of a movie for leading axons ( $n=10$ ) and follower axons. In the later case only axons with clearly discernible filopodia were chosen ( $n=8$ ).

### Data analysis

Quantitative axon growth rates data was analyzed to test for significant differences using Student's  $t$ -test analyses with Origin software. In cases where one average growth rate was compared with two different growth rates the  $P$  value was corrected for multiple comparisons.

## Results

### gata2::GFP labels a specific neuronal cluster of the forebrain

Neuronal differentiation and axonogenesis in the zebrafish

forebrain have been shown to begin between 17-28 hpf (Chitnis and Kuwada, 1990; Wilson et al., 1990; Ross et al., 1992). The relative arrangement of the early neuronal clusters inside the brain and their tracts, deduced from antibody staining against the neuron specific acetylated alpha tubulin (Chitnis and Kuwada, 1990; Wilson et al., 1990; Ross et al., 1992), is schematically illustrated (Fig. 1A,B). To permit reproducible *in vivo* imaging, we employ a stable transgenic line in which the cis-regulatory domain of the transcription factor GATA2 drives GFP (*gata2::GFP*) (Meng et al., 1997), and shows early expression in the earliest differentiating cells in the forebrain (Fig. 1C,D). The GFP-positive cells, 8-10  $\mu\text{m}$  in diameter, form bilateral clusters in the ventral forebrain that extend along the optic recess from the anterior diencephalon towards the ventral flexure (Fig. 1C,D). Staining with acetylated alpha tubulin antibody at 18-28 hpf reveals two distinct clusters of acetylated alpha tubulin-positive ventrorostral cluster (vrc) neurons (red); many of these cells express GFP (green) (Fig. 1E). By 24 hpf, all vrc neurons express GFP (Fig. 1F).

### The first axons to form the POC are *gata2::GFP* positive

Immunohistochemistry with the acetylated alpha tubulin (AT) antibody shows that the postoptic commissure (POC) is set up between 21 and 23hpf (Fig. 2A-D). In addition to labeling the axons of the early neuronal scaffold, AT also labels the cell bodies of cells undergoing axonogenesis, ependymal processes and cilia (Chitnis and Kuwada, 1990), as well as the superficial network of nerve fibers running just beneath the ectoderm. At the early stages of POC formation these labeled processes are closely juxtaposed and can appear as axon-like processes. Thus, our detailed analyses of the earliest POC axons were performed on individual optical sections.

Double-labeling studies show that these earliest axons of the POC, detected by AT, are GFP positive. At 21 hpf, no axonal staining with either AT or GFP can be seen along the future POC trajectory except for the cell bodies and ependymal processes of delaminating neuroepithelial cells (Fig. 2E). At 23 hpf a small number of axons slightly beneath the surface ectoderm are visible across the POC (Fig. 2F). Analysis and rendering of these double labeled preparations is often challenging because the GFP expression levels in axons are weak after fixation. To confirm that all of the initial axons growing across the POC are GFP positive, we employed spectral analysis using a Zeiss LSM-510 META microscope. Given the low levels of GFP expression, some axons appear reddish in the double overlay, even though they express distinct GFP fluorescence. Analysis of the individual *z* sections further confirms that both ependymal processes and superficial nerve fibers extend near the commissural axons and these do not express GFP. At later stages, more GFP positive axons appear (Fig. 2H), as well as a small number of axons that do not express GFP, probably originating from other neuronal clusters as previously described (Wilson and Easter, 1991).

DiI-labeling experiments were performed to confirm that the first GFP axon is the first axon along the future POC tract. Transgenic *gata2::GFP* fish were timelapsed until the first GFP-expressing growth cone appeared (Fig. 3A), at which time the embryos were fixed briefly to retain GFP and growth cone morphology. DiI injection into the vrc cluster (Fig. 3C) reliably labeled the first GFP-expressing axon including its growth cone; no DiI-labeled axons were visible ahead of the leading GFP-positive process (Fig. 3B). Thus, the first GFP-positive axon is the initial axon that grows along the POC trajectory.

### Axon kinetics during POC formation *in vivo*

To characterize the growth behavior of POC axons, we performed a series of time-lapse confocal microscopy experiments ( $n=22$ ) using *gata2::GFP* zebrafish embryos. At 22-23 hpf, one to three discernable axons from the bilateral vrcs advance rostrally along the POC path (Fig. 4A). Within 1 hour, these axons meet, creating a continuous axon arc along the future POC trajectory (the early axon from the right is indicated with pink arrow in Fig. 4A,B). Later axons from both sides (blue arrows in Fig. 4A-D) fasciculate with the initial axons at various points along the commissure and follow

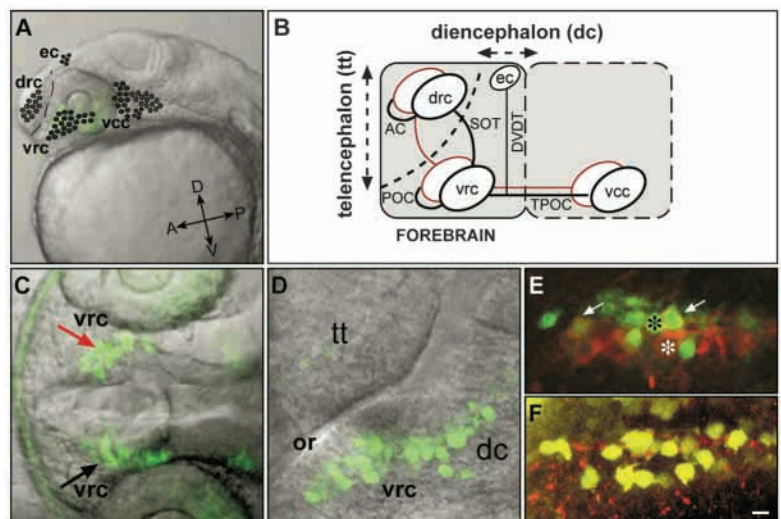


**Fig. 1.** Zebrafish forebrain primary neuronal scaffold contains *gata2::GFP*-positive neurons. (A) 24 hpf zebrafish transmitted light view. The approximate location of the early neuronal clusters in the forebrain are schematically shown. (B) Schematic drawing illustrating the position of the major neuronal clusters and the axon tracts that connect them in the anterior CNS in zebrafish (based on Chitnis and Kuwada, 1990; Wilson et al., 1990; Ross et al., 1991). (C,D) Confocal images of dorsal (C) and lateral (D) views of a 24 hpf *gata2::GFP* zebrafish showing the location of GFP-positive cells in relation to forebrain morphology. The cells are located bilaterally (C) and occupy the rostroventral part of the diencephalon along the optic recess (or) (D). (E,F) Fluorescent confocal images showing the vrc stained with acetylated alpha tubulin antibody (red) to reveal the identity of *gata2::GFP*-expressing cells (green). White asterisk indicates a vrc cell with little or no GFP; black asterisk marks a GFP-positive vrc cell. White arrows indicate cells where colocalization of the neuronal antibody and the GFP can be seen (E). At 24 hpf all vrc cells express GFP and appear yellow due to spectral overlap between the green GFP and the neuronal antibody (F). Scale bar: 80  $\mu\text{m}$  in A; 20  $\mu\text{m}$  in C; 10  $\mu\text{m}$  in D-F. tt, telencephalon; dc, diencephalon; drc, dorsorostral cluster; vrc, ventrorostral cluster; vcc, ventrocaudal cluster; ec, epiphysial cluster; SOT, supraoptic track; TPOC, track of postoptic commissure; POC, postoptic commissure; AC, anterior commissure; or, optic recess.

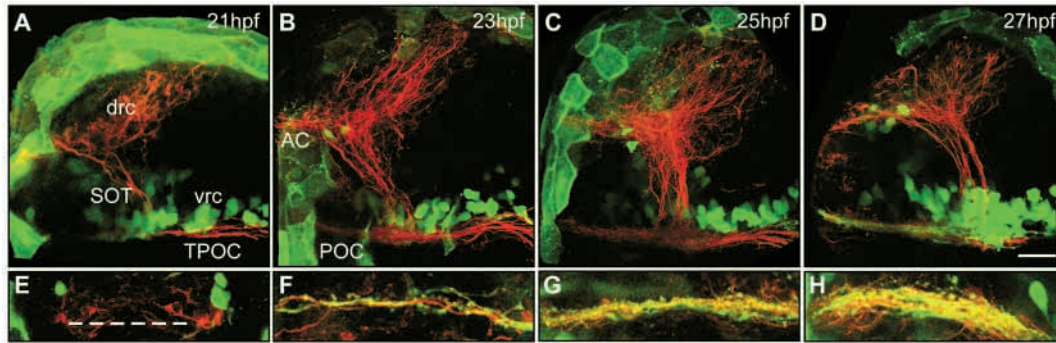


**Fig. 2.** *gata2::GFP*-positive axons pioneer the POC and also mark the majority of later POC axons. *Gata2::GFP* cells and their axons are depicted in green and the primary neuronal scaffold in red. Rostral is towards the left and dorsal is towards the top. Images are maximum intensity projection (MIP) views of confocal *z* stacks. (A-D) Lateral images at 21, 23, 25 and 27 hpf showing the relative position of *gata2::GFP* cells (green) with respect to the neuronal scaffold revealed with acetylated alpha tubulin (red). (E-H) Corresponding frontal views of the POC show *gata2::GFP*-expressing axons pioneer the POC. At 21 hpf, only early neurons differentiating away from the neuroepithelium can be seen, but no axons are present where the POC will form (broken white line) (E). At 23 hpf, a small number of axons can be seen across the POC; these early axons express GFP although because of fixation some of the GFP signal is too weak to be visible in the overlay image (F). At 25 and 27 hpf, respectively, the POC thickens. *GFP*-positive axons can be seen spanning the entire width of the commissure (G,H). The small number of axons that appear to not express GFP reflects axons from other brain regions that project their axons along this tract. Scale bar: 20  $\mu\text{m}$ .

them across the midline (see Movie 1 at <http://dev.biologists.org/supplemental/>).

These movies reveal two distinct classes of behaviors. The first axon that emerges maintains its leading position towards the midline and across it (Fig. 4A,B, pink arrow); the trailing axons stay close behind, crossing the midline after the first axon crosses (Fig. 4C,D, blue arrow). To analyze the dynamics of axons along the POC trajectory, length and position along

the POC trajectory was measured at every time point for each axon visible in our timelapse recordings. To allow easier comparison of axon behaviors, axon growth was plotted as distance from midline along the POC trajectory as a function of time (Fig. 4E). At the midline, the first visible axon (pink line) has an almost flat slope, signifying that this axon slows down in this region (pink boxed area). By contrast, a later axon (blue line) has a continuous, steep slope at the midline (blue boxed area) showing that it does not slow down. Thus the two types of axons show different behaviors at the midline, an important intermediate target for commissural axons (Kaprielian et al., 2001).

### POC axon nomenclature

In view of the order in which the axons reached and crossed the midline, we have defined the first axon from either side to cross the midline as a leader axon; all later axons observed along the POC are defined as follower axons. In 25% of the cases, axons originating from the two opposite vrcs arrived at the midline at approximately the same time and both were defined as leader axons. In the rest of the cases, one axon arrived early at the midline and grew across it. In these cases, the initial axon was defined as a leader and the contralateral axon was defined as a follower.

### Quantitative analysis of leader and follower axons reveals differences in their behavior at the midline

Quantitative analysis of POC axons ( $n=46$ ) reveals a behavioral difference between leader and follower axons in the midline region ( $\pm 10 \mu\text{m}$  from the midline). Within this region, leading axons slow significantly (Fig. 5A) compared with follower axons (Fig. 5B), correspondingly their average slopes in this region are markedly different. This difference is robust: the difference between leader and follower axon behavior at the midline is maintained even when they are averaged (Fig. 5C). The extended time that leading axons spend within the midline region is due to a more than 50% reduction in growth by the

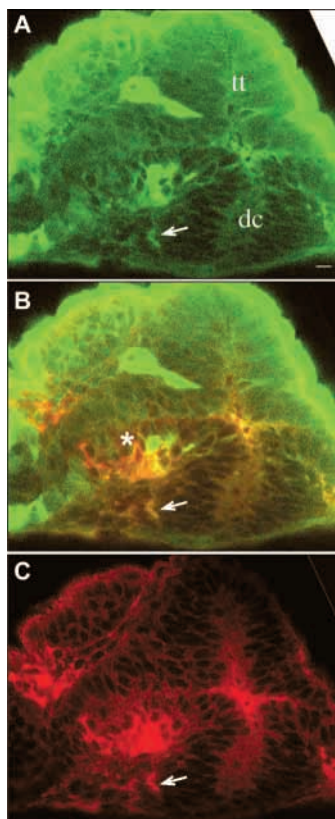


**Fig. 3.** DiI filled *gata2::GFP*-positive vrc cluster where first *GFP* axon has just started to grow to midline shows no red axons ahead of the *GFP*. *gata2::GFP* embryo fixed immediately after the first *GFP*-positive axon began growing to midline and the vrc cluster (asterisk) was filled with DiI to label axons from the vrc. (A) Front view of the green channel showing the *GFP*-positive vrc cells and the first *GFP*-expressing growth cone (arrow) projecting towards the midline. (B) Merged green and red emission channels showing the injected vrc cluster (asterisks) and the labeled growth cone (arrow). No other DiI filled axons are visible ahead of the *GFP*-expressing axon. (C) Red channel showing the DiI fill and the labeled DiI growth cone (arrow). Scale bar: 10  $\mu\text{m}$ .

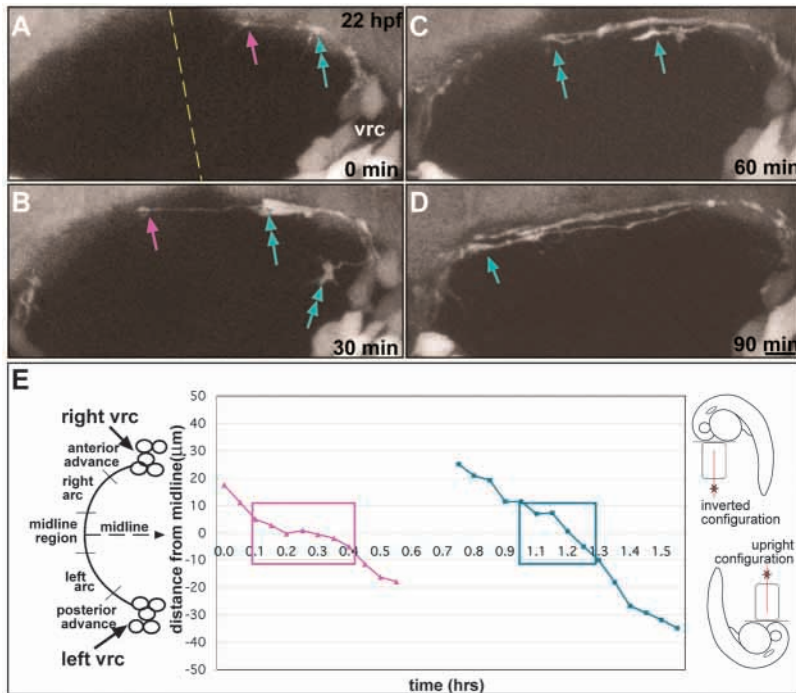


**Fig. 4.** Timelapse imaging of a wild-type *gata2::GFP* growth cones crossing the ventral forebrain and forming the POC. (A-D) Selected images of single time points from one 3 minute interval timelapse sequence showing a typical leading growth cone (pink arrows in A and B) from the vrc cluster navigating towards and past the midline, where it is joined by the growth cone from the opposite cluster (not visible in B because it is masked by fluorescence from more dorsal sections). Subsequently, later growth cones (blue arrows in B-D) also cross the midline and grow across the POC. The midline is indicated by a broken line; time is shown in minutes. Scale bar: 10  $\mu\text{m}$ . (E) A typical distance from midline along the POC trajectory axon plot. Axon length at each time point is plotted as distance from midline along the POC trajectory. The leading growth cone is plotted in pink and a later (follower) axon is plotted in blue corresponding to the growth cones marked with pink and arrows in A-D. The axons shown here start from the right vrc (top of the plot) and cross over to the left vrc (bottom of the plot) as indicated in the schematic to the left of the graph. The two axons advance across the midline with different rates as indicated by the slope of each line (see pink and blue boxed regions). On the right, two microscope configurations show how the imaging was performed. The timelapse shown in A-D was obtained in the inverted configuration.

leader axons at the midline. At the midline, leader axons grow at an average rate of  $35 \pm 5 \mu\text{m}/\text{hour}$  as opposed to  $85 \pm 5 \mu\text{m}/\text{hour}$ , the average growth rate of leader axons along the rest of the POC trajectory (Fig. 5D). Follower axons do not display this behavior; their average growth rates inside ( $91.6 \pm 7.1 \mu\text{m}/\text{hour}$ ) and outside ( $93.7 \pm 6.2 \mu\text{m}/\text{hour}$ ) are equivalent (Fig. 5D). Thus, leader and follower axons grow at comparable rates outside the midline region, but display drastically different growth rates near the midline.

### Both slower speeds and higher frequency of retractions contribute to lower average growth

Axon growth rate reflects both the absolute speed and direction of growth. Thus, two factors could contribute to the apparent slowing of leader axons at the midline: (1) a decrease in axon growth speed and (2) higher number of growth cone retractions around the midline without a necessary reduction in growth speed. To examine the relative importance of these two factors, we determined the frequency of brief retractions of the leader and follower growth cones within the midline region and outside of it. Ninety percent of leader axons displayed retraction behavior at the midline; by contrast, only 15% of follower axons showed retraction in this region. When higher retraction frequency was compensated for, the resulting average absolute growth rate for leading axons was still significantly lower at the midline ( $58 \pm 9.2 \mu\text{m}/\text{hour}$ ) compared with followers ( $97 \pm 5.3 \mu\text{m}/\text{hour}$ ) (Table 1). Outside the midline, leader and follower growth cones retracted with similar low frequencies and their average growth rates do not change significantly, even when we account for these retractions (Table 1).

### Leader and follower axons differ in growth cone morphology

Our time-lapse imaging allowed us to resolve entire growth cone shapes along with a number of filopodia for all leader

growth cones and a fraction of follower growth cones (Fig. 6A-C). To test if growth cones of leader and follower axons differ in complexity, we computed width/length (w/l) ratios for the two classes of axons. Leading growth cones (Fig. 6A,B, long pink arrow) were consistently wider and shorter (higher w/l ratio) than the elongated shape of the follower growth cones (Fig. 6B,C, long blue arrow). At the midline, leader growth cone w/l ratios ( $0.43 \pm 0.2$ ,  $n=12$ ) were 50% larger than follower growth cone w/l ratios ( $0.24 \pm 0.1$ ,  $n=8$ ) (Fig. 6D). The average growth cone areas for leader and follower axons did not differ (Fig. 6E), consistent with what has been found in growth cones of corticothalamic projections in ferrets and cats (Kim et al., 1991). In the midline region, leading axons had up to 50% more filopodia than the follower axons (average filopodia length did not differ). The filopodia on leaders were arranged at all angles to the growth cone (see Fig. 6A, short pink arrows); by contrast, the filopodia of follower axons were mostly oriented in a forward direction (Fig. 6A, short blue arrows). Together, these data show that the growth cones of leader and follower axons display marked differences as judged by the different w/l ratios and number and orientation of their filopodia.

### Direct interaction between leader and follower axons

Because follower axons grew in close contact with the leader axon and had different midline kinetics, we examined how the presence of the leader axon affects follower axons in vivo. For this purpose, we examined follower axons in samples where the leader axon was damaged by intense laser light. Repeated high laser illumination of single leader growth cones to the point of saturation causes permanent damage to single axons and has been used as a tool to ablate cells and their processes (Pike et al., 1992; Mayers and Bastiani, 1993). Strong laser illumination over three to five consecutive time points resulted in leader axons whose growth cones rounded up and did not recover ( $n=3$ ; Fig. 7A). After the growth cone of the leader was

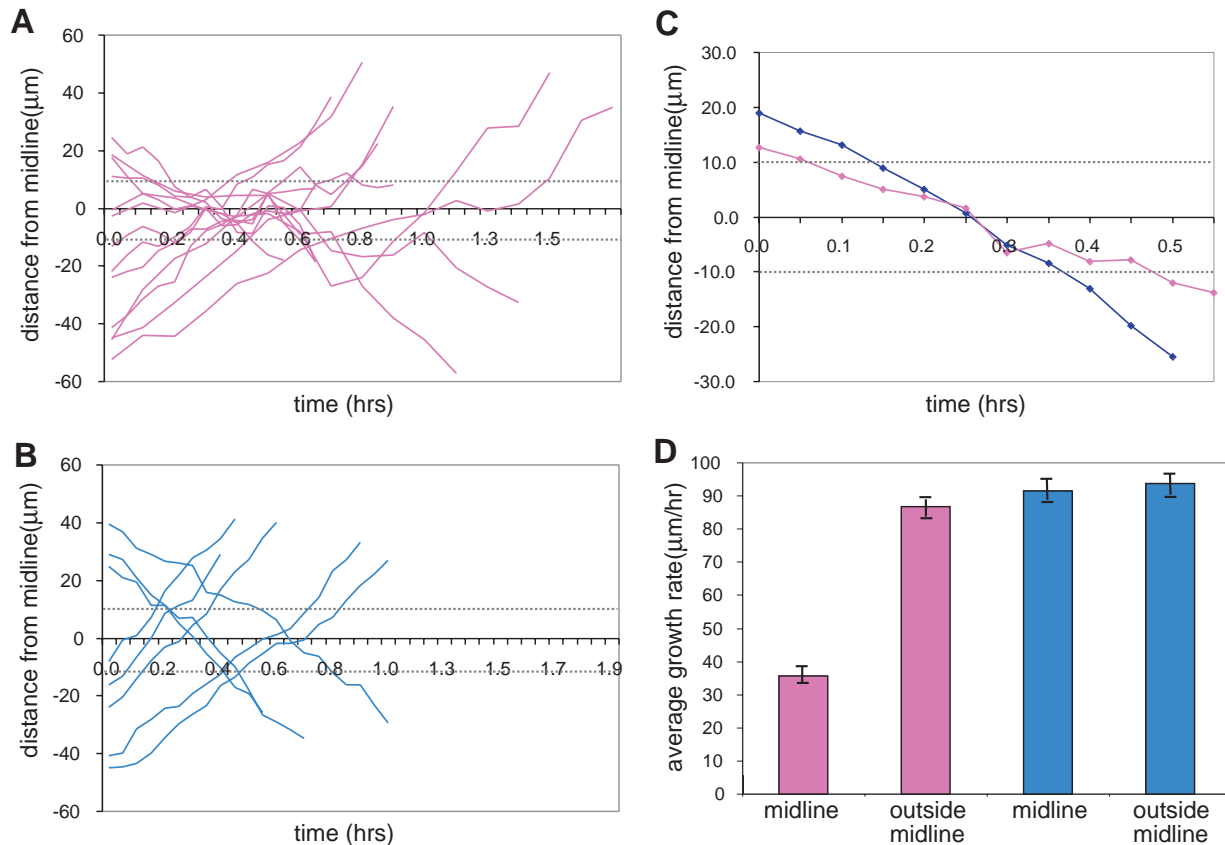


**Fig. 5.** POC axon dynamics with respect to the midline. Quantitative analysis of axon growth rates reveals a difference in axon behavior around the midline not readily apparent from direct observation of timelapse experiments. (A,B) Representative plots of distance from the midline along the POC trajectory versus time for leader (A) and follower (B) axons. Leader axons spend longer time within  $\pm 10\mu\text{m}$  of midline (broken black line in A-C), while the growth of later axons does not slow down in this region. (C) Average behavior of leader ( $n=16$ ) and follower ( $n=24$ ) axons at the midline. Leader and follower axon plots were centered on the timepoint when each axon crossed the midline. The average plot shows a more than twofold difference between the time leader and follower axons stay at the midline. Individual plots of all axons from the left vrc were reflected around the  $x$ -axis. (D) Average growth rates  $\pm$  s.e.m. for leader (pink) and follower (blue) axons with respect to the midline and outside midline region. Leading axons grow significantly more slowly at the midline compared with their average growth rate away from midline and compared with follower axons at the midline ( $P < 0.001$ , Student's  $t$ -test corrected for multiple comparison).

damaged and collapsed *in vivo* at or before the midline (Fig. 7A, pink arrow with an asterisk, see Fig. 7 and Movie 2 at <http://dev.biologists.org/supplemental/>), the nearest follower axon changed its behavior and slowed down within the midline region (Fig. 7A, blue arrow with an asterisk), while later follower axons behaved as they normally would (i.e., crossed the midline swiftly). Thus, early POC axons can adopt leader-characteristic midline behavior. As long as one axon becomes

a leader, subsequent axons that grow along this tract behave as followers at the midline.

### Axon fasciculation can explain the differences between midline kinetics of leader and follower axons

Leader axons slow down at the midline because they must interpret and navigate through a complex environment of

**Table 1. Longer midline interaction for leader axons is due to decrease in speed as well as higher frequency of retraction in leader axons**

	$n$	Midline		Away from midline	
		Average ( $\mu\text{m}/\text{hour}$ )	Absolute ( $\mu\text{m}/\text{hour}$ )	Average ( $\mu\text{m}/\text{hour}$ )	Absolute ( $\mu\text{m}/\text{hour}$ )
Leader	17	$35.6 \pm 4.5^{*,\dagger}$	$58.2 \pm 9.2^{*,\dagger}$	$86.9 \pm 6.9^*$	$95.3 \pm 5.7^*$
Follower	22	$91.6 \pm 7.1^\dagger$	$97 \pm 5.3^\dagger$	$93.7 \pm 6.2$	$102.9 \pm 9.9$

Mean  $\pm$  s.e.m. of average growth rates and absolute growth rates for leader and follower axons at and away from the midline. To ensure that different leader and follower axon retraction frequency did not vary with our sampling interval, timelapse data were collected at 1.5, 3 and 6 minute intervals. The table above is based on pooled data, as similar retraction percentages for both classes of axons were obtained independent of the sampling interval. The growth rates, either compensated for the increased retractions (absolute growth) or not (average growth) are slower at the midline for leaders ( $*P < 0.001$ , Student's  $t$ -test). Similarly, the growth rates of the leaders are slower than follower axons at the midline ( $^\dagger P < 0.001$ , Student's  $t$ -test).

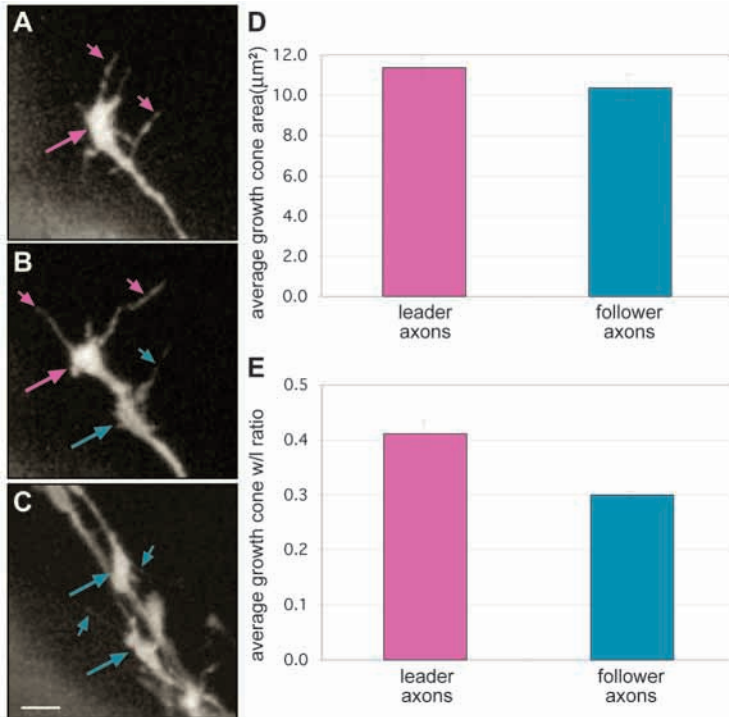
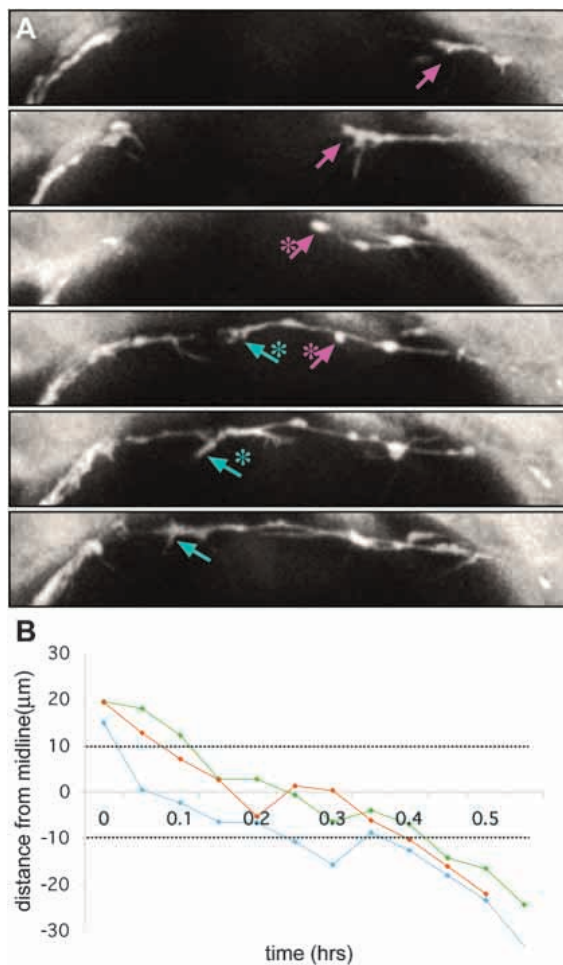


**Fig. 6.** Growth cone morphology analysis for POC axons. Growth cone morphology can be visualized during timelapse imaging of the POC axons. (A-C) Representative growth cones of leader (long pink arrow) and follower (long blue arrow) axons are shown. Filopodia present on both types of growth cones are also indicated with smaller arrows (pink for leader and blue for follower). Scale bar: 10  $\mu\text{m}$ . (D) Average growth cone areas do not differ between leader ( $n=12$ ) and follower ( $n=8$ ) axons. Only clearly visible follower axons were chosen for this analysis. (E) Average width to length (w/l) ratio plot shows a significantly higher ratio for leader axons ( $n=12$ ) compared with follower axons ( $n=8$ ) ( $P<0.05$ , Student's  $t$ -test).



positive and negative midline cues. As follower axon growth cones can use leaders as guides to cross the midline, they are less exposed to midline signals allowing them to cross the midline swiftly. Thus, a simple difference in growth cones exposure to local cues can explain the difference between leader and follower axon kinetics at the midline. Both growth cone morphology differences and the ablation experiments support this model. To test this hypothesis further, we turned to an experiment in nature. As mentioned earlier, in 75% of the cases, a leader axon from one side crosses the and the contralateral first axon grows along the leader across the midline displaying fast midline kinetics. As leader and follower growth cone morphology differences correlate with their midline kinetics, we examined growth cone morphology of these contralateral axons before and after they encountered the leader axon. If fasciculation of the growth cone with the leader axon alters its interaction with the environment,

**Fig. 7.** In the absence of a leader axon, follower axons grow more slowly at the midline. (A) Single time point images showing a leader axon (pink arrow) that projects towards the midline and is injured right before crossing it (pink arrow with asterisk). A follower axon behind it (blue arrow) overtakes the leader axon and crosses the midline (blue arrow with asterisk). After this axon crosses the midline another axon from the left vrc also grows across the midline. The two growth cones: the new leader from the right vrc (blue arrow with asterisk) and the first axon from the left vrc have just undergone their stereotypic behavior and are not aligned with the POC trajectory until the last image where their growth cones establish contact with the opposite axon shaft. (B) Axon distance from midline along the POC trajectory graph showing three separate cases where follower axon was analyzed after the leader axon was damaged. The axon graphed in blue corresponds to the follower axon shown above (blue arrow in A).

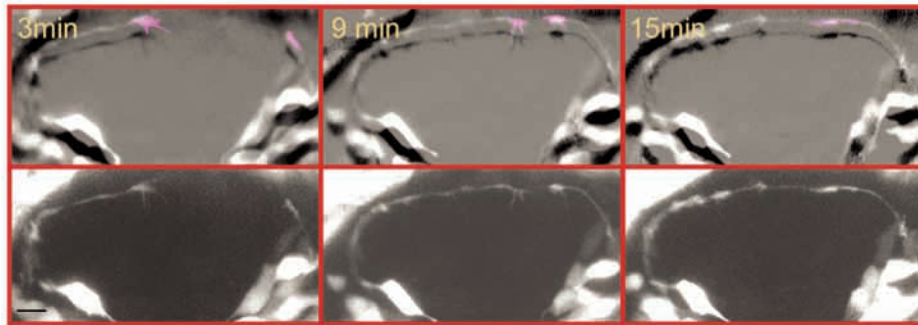


**Fig. 8.** Leader axon alters midline kinetics of first contralateral axon at the midline during commissure formation. Single time point images showing stereotypic interaction between the initial POC growth cones. Two growth cones, one from each side, are visible with one already at the midline (left). Up to this point both growth cones have complex morphologies. Upon contact, however (middle panel), both growth cones change shape and become elongated (right) even though the second growth cone has not yet crossed the midline. When this second axon grows across, it has fast midline kinetics similar to a follower axon. Scale bar: 10  $\mu\text{m}$ .

resulting in faster growth at the midline, then we would expect to see a growth cone morphology change in the contralateral axon accompanying the fast kinetics we observe in these cases. This change would be expected to occur even before the growth cone crosses the midline simply because it now grows along another axon. Following initial contact with a leading axon that has crossed the midline, growth cones of contralateral axons undergo a drastic change in shape from complex to elongated even before they themselves cross the midline (Fig. 8, see Movie 3 at <http://dev.biologists.org/supplemental/>). Thus, simple growth cone shape change brought about by the newly available opposite commissural axon substrate can switch the midline kinetics of these axons from leader to follower.

## Discussion

Here, *in vivo* microscopy of embryonic zebrafish expressing GFP in the ventrorostral clusters (vrcs) of cells in the embryonic forebrain permits the early events involved in establishing the postoptic commissure (POC) to be followed. The labeled cells in the *gata2::GFP* fish send their axons along the POC earlier than any others (22–23 hpf). As the initial axons course towards the midline, one of them becomes the leader axon, approaching and crossing the midline first. After a characteristic slowing at the midline, the two leader axons pass one another and continue on towards their contralateral targets. Later axons follow the leaders but do not overtake them or behave like them at the midline. Thus, the leading axons from the vrcs are in the correct place and show the correct behaviors to serve as the early pioneers of the POC.

Commissural axons have been studied in invertebrates (Myers and Bastiani, 1993; Boyan et al., 1995) and in vertebrate spinal cord (Bovolenta and Dodd, 1990), and appear to share similar mechanisms for building the early neuronal scaffold. However, little is known about commissural axon kinetics during early brain development in vertebrates *in vivo*. Our dynamic imaging results show behaviors that might not have been expected from invertebrate studies. First, we find that follower axons can adopt a pioneering role if the leader is eliminated, contrary to the case in invertebrates where defined pioneer(s) play a central role in guiding later axons to their targets (Raper et al., 1984; Klose and Bentley, 1989; Gan and Macagno, 1994; Hidalgo and Brand, 1997). Consistent with

these data, removal of some of the primary motoneurons in the zebrafish spinal cord does not affect the establishment of correct projections in the remaining population of primary axons (Pike and Eisen, 1990). This suggests that the vrc cells that send their axons along the early POC act as an equivalence group, with only one or two of the axons serving as leaders. The signals that promote the leaders or that permit leaders to suppress leader behavior in followers have yet to be defined. Second, unlike invertebrates, where bilateral homologues of early commissural axons arrive at the midline together (Myers and Bastiani, 1993; Boyan et al., 1995), and where cooperative fasciculation between contralateral homologues of commissural axons appears to be essential for allowing each axon to cross the midline (Myers and Bastiani, 1993), we find that this is not always the case in zebrafish POC formation. In 75% of the timelapses ( $n=22$ ), an initial axon emerging from one of the ventral clusters arrived at and crossed the midline before the contralateral axon got within 15–20  $\mu\text{m}$  of the midline, suggesting that leader axons can navigate the midline territory alone. Furthermore, although contralateral Q1 commissural growth cones in grasshopper exhibit strong affinity for each other at the midline (Myers and Bastiani, 1993), growth cones of leading POC axons do not appear to have equally high affinity for each other. Contact of leader axon growth cones via their filopodia makes one or both growth cones jog to the side so that rather than facing each other they are parallel to each other. As they advance forward, each growth cone makes contact with the opposite axon shaft directly behind its growth cone, and then follows it to the other side to establish the initial POC axon fascicle (data not shown).

Direct interaction between axons has been suggested to influence follower axon growth direction and growth cone morphologies in retinal ganglion cells *in vitro* (Devenport et al., 1999). We report a clear behavioral consequence for axons following an already established track that can be seen in terms of their growth cone morphology and their midline kinetics *in vivo*. Similar, growth cone morphology differences between the initial and later axons have been noted in invertebrates (LoPresti et al., 1973; Raper et al., 1984) and in fixed tissues in vertebrate systems (Kim et al., 1991; Wilson and Easter, 1991). We find that axon kinetics and growth cone morphology correlates with whether the axon is a pioneer or a follower. The fact that upon elimination of a leader axon, follower axons

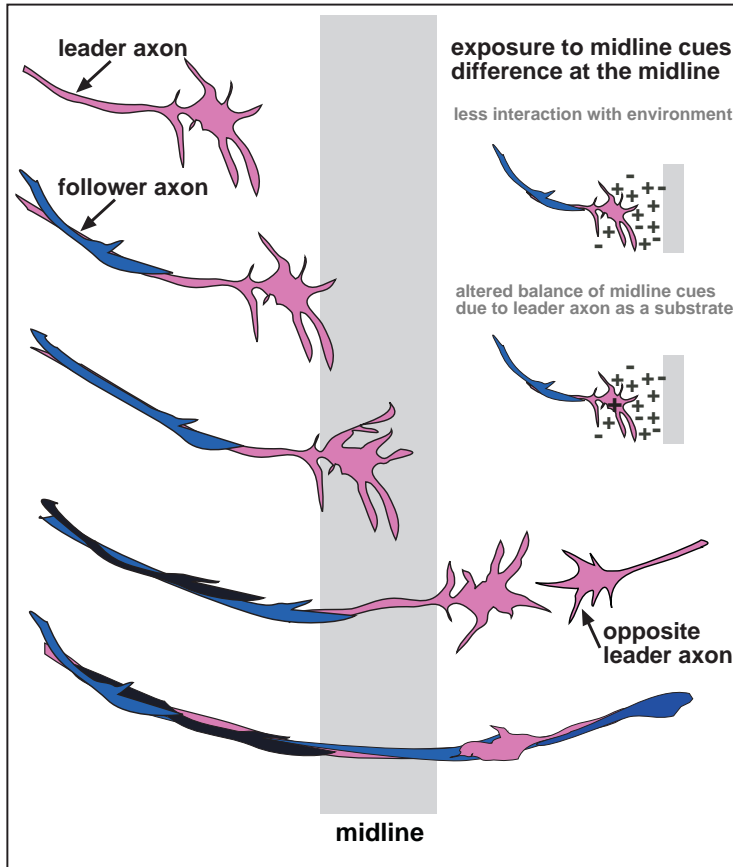


**Fig. 9.** How fasciculation between commissural axons alters their midline kinetics. A schematic drawing shows a leader axon (pink) and a number of follower axons (blue and black) growing through the midline. The leading axon being the first, is completely exposed to the guidance cues in the environment. Its growth cone must sense all the positive and negative midline cues and interpret them accordingly, which results in slow kinetics of leader axons at the midline where these cues are found. By growing along the leader, follower axons are less exposed to midline cues. This can happen because their growth cones are shaped differently, which limits their exposure to conflicting midline signals and/or because the substrate that the leader axon provides contributes an extra signal that allows them to grow across the midline swiftly.

fasciculation would speed the kinetics of followers through the midline milieu, skewing the balance more sharply and resulting in less retractions and pausing. In either scenario, leader-follower axon fasciculation ensures that all commissural axons stay sensitive to the midline cues but permits later axons to cross the midline swiftly and expedite commissure formation.

Studies in invertebrates and vertebrates strongly suggest that midline cells play an important role in axon guidance (Hatta, 1992; Colamarino and Tessier-Lavigne, 1995; Greenspoon et al., 1995; Matise et al., 1999). Mutations affecting midline signaling (Varga et al., 2001) or the presence of midline cells (Pike and Eisen, 1990; Varga et al., 2001) result in axon pathfinding defects. The present focus on the complex midline domain has assumed that all axons react similarly to these positive and negative cues, thus slowing down at the midline (Bovalenta and Dodd, 1990; Mason and Wang, 1997). Our demonstration that axon kinetics are shaped by an ongoing interaction between leader and follower axons, in addition to any midline cues, highlights the importance of investigating the molecular underpinnings of midline crossing in vertebrates in vivo.

We thank Andres Collazo and Olivier Bricaud for suggesting the *gata2::GFP* line as candidate for our work as well as Shuo Lin for the *gata2::GFP* adults. We thank Kai Zinn, Reinhard Köster, Cyrus Papan and Helen McBride for discussions and critical reading of the manuscript. This work was supported by NIH RO1 HD043897.

## References

- Bate, C. M. (1976). Pioneer neurons in an insect embryo. *Nature* **260**, 54-56.
- Bastiani, M., Raper, J. A. and Goodman, C. S. (1984). Pathfinding by neuronal growth cones in grasshopper embryos: III. Selective affinity of the G growth cone for the P cells within the A/P fascicle. *J. Neurosci.* **4**, 2311-2328.
- Bentley, D. and Keshishian, H. (1982). Pathfinding by peripheral pioneer neurons in grasshoppers. *Science* **218**, 1082-1087.
- Bovalenta, P. and Dodd, J. (1990). Guidance of commissural growth cones at the floor plate in embryonic rat spinal cord. *Development* **109**, 435-447.
- Boyan, G., Therianos, S., Williams, L. D. and Reichert, H. (1995). Axogenesis in the embryonic brain of the grasshopper *Schistocerca gregaria* an identified cell analysis of early brain development. *Development* **121**, 75-86.
- Chitnis, A. B. and Kuwada, J. Y. (1990). Axonogenesis in the brain of zebrafish embryos. *J. Neurosci.* **10**, 1892-1905.
- Chitnis, A. B. and Kuwada, J. Y. (1991). Elimination of a brain track increases errors in pathfinding by follower growth cones in the zebrafish embryo. *Neuron* **7**, 277-285.

change their midline kinetics, and that simple interaction between bilateral leader axons can alter their growth cone shape and midline kinetics, demonstrates that pioneering axons and the early follower axons growing along them interact with one another in vivo. Although it remains possible that these interactions are indirect, through the leader altering the midline environment, we favor the interpretation that the difference in kinetics results from direct interaction between these axons.

One way this might work is that fasciculation between the follower growth cones and the leader axon simply changes their exposure to the positive and negative growth signals found at the midline (Fig. 9). In support of this model, we observe that only the initial leader axon that pioneers a commissure displays drastic slowing at the midline and has a complex growth cone. Later axons following this pioneer do not show the same complex growth cone morphology, nor do they slow down at the midline. This model predicts that when the leader is ablated, the substrate it provides for the next axon is removed, and the next axon becomes more exposed to the environmental cues. As a result its growth cone morphology as well as its midline kinetics change to that of a pioneer as observed. Similarly, contralateral leading axons upon fasciculation change their growth cone morphology and midline kinetics to that of followers even before crossing the midline as would be expected from this model. It is also possible that the differences reported here, result from the balance between positive and negative midline cues that growth cones interpret, as characterized in vitro in several studies of growth cone guidance (Song and Poo, 1999). In this case, axon

- Chitnis, A. B., Patel, C. K., Kim, S. and Kuwada, J. Y.** (1992). A specific brain track guides follower growth cones in two regions of the zebrafish brain. *J. Neurobiol.* **23**, 845-854.
- Colamarino, S. A. and Tessier-Lavigne, M.** (1995). The role of the floor plate in axon guidance. *Annu. Rev. Neurosci.* **18**, 497-529.
- Devenport, R. W., Thies, E. and Cohen. M. L.** (1999). Neuronal growth cone collapse triggers lateral extensions along trailing axons. *Nat. Neurosci.* **2**, 254-259.
- Dynes, J. and Ngai, J.** (1998). Pathfinding of olfactory neuron axons to stereotyped glomerular targets revealed by dynamic imaging in living zebrafish embryos. *Neuron* **20**, 1081-1091.
- Gan, W.-B. and Macagno, E. R.** (1995). Developing neurons use a putative pioneer's peripheral arbor to establish their terminal fields. *J. Neurosci.* **15**, 3254-3262.
- Greenspoon, S., Patel, C. K., Hashmi, S., Bernhardt, R. R. and Kuwada, J. Y.** (1995). The notochord and floor plate guide growth cones in the zebrafish spinal cord. *J. Neurosci.* **15**, 5956-5965.
- Hatta, K.** (1992). Role of the floor plate in axonal patterning in the zebrafish CNS. *Neuron* **9**, 629-642.
- Hidalgo, A. and Brand, A. H.** (1997). Targeted neuronal ablation: the role of pioneer neurons in guidance and fasciculation in the CNS of *Drosophila*. *Development* **124**, 3253-3262.
- Hutson, L. D. and Chien, C.** (2002). Pathfinding and error correction by retinal axons: the role of *astray/robe2*. *Neuron* **33**, 205-221.
- Jacobs, J. R. and Goodman, C. S.** (1989). Embryonic development of axon pathways in the *Drosophila* CNS: IV. Behavior of pioneer growth cones. *J. Neurosci.* **9**, 2412-2422.
- Jontes, J. D., Buchmanan, J. and Smith, S. J.** (1999). Growth cone and dendrite dynamics in zebrafish embryos: early events in synaptogenesis imaged *in vivo*. *Nat. Neurosci.* **3**, 231-237.
- Kaprielian, Z., Runko, E. and Imondi, R.** (2001). Axon guidance at the midline choice point. *Dev. Dynamics* **221**, 154-181.
- Kim, G. J., Shatz, C. J. and McConnell, S. K.** (1991). Morphology of pioneer and follower growth cone in the developing cerebral cortex. *J. Neurobiol.* **22**, 629-642.
- Klose, M. and Bentley, D.** (1989). Transient pioneer neurons are essential for formation of an embryonic peripheral nerve. *Science* **245**, 982-983.
- LoPresti, V., Macagno, E. R. and Levinthal, C.** (1973). Structure and development of neuronal connections in isogenic organisms: cellular interactions in the development of the optic lamina of *Daphnia*. *Proc. Natl. Acad. Sci. USA* **70**, 433-437.
- Mason, C. A. and Wang, C.** (1997). Growth cone form is behavior-specific and, consequently position-specific along the retinal axon pathway. *J. Neurosci.* **17**, 1086-1100.
- Mastick, G. S. and Easter, S. E., Jr** (1996). Initial organization of neurons and tracks in the embryonic mouse fore and midbrain. *Dev. Biol.* **173**, 79-94.
- Matise, M. P., Lustig, M., Sakurai, T., Grumet, M. and Joyner, A. L.** (1999). Ventral midline cells are required for the local control of commissural axon guidance in the mouse spinal cord. *Development* **126**, 3649-3659.
- McConnell, S. K., Ghosh, A. and Shatz, C. J.** (1989). Subplate neurons pioneer the first axon pathway from the cerebral cortex. *Science* **245**, 978-981.
- Meng, A., Tang, H., Ong, B. A., Farrell, J. and Lin, S.** (1997). Promoter analysis in living zebrafish embryos identifies a cis-acting motif required for neuronal expression of GATA-2. *Proc. Natl. Acad. Sci. USA* **94**, 6267-6272.
- Myers, P. Z. and Bastiani, M. J.** (1993). Growth cone dynamics during the migration of an identified commissural growth cone. *J. Neurosci.* **13**, 127-143.
- Pike, S. H. and Eisen, J.** (1990). Identified primary motoneurons in embryonic zebrafish select appropriate pathways in the absence of other primary motoneurons. *J. Neurosci.* **10**, 44-49.
- Pike, S. H., Melancon, F. and Eisen, J.** (1992). Pathfinding by zebrafish motoneurons in the absence of normal pioneer axons. *Development* **114**, 825-831.
- Raper, J. A., Bastiani, M. and Goodman, C. S.** (1984). Pathfinding by neuronal growth cones in grasshopper embryos: IV. The effects of ablating the A and P axons upon the behavior of the G growth cone. *J. Neurosci.* **4**, 2329-2345.
- Ross, L. S., Parrett, T. and Easter, S. S.** (1992). Axonogenesis and morphogenesis in the embryonic zebrafish brain. *J. Neurosci.* **12**, 467-482.
- Song, H. and Poo, M.** (1999). Signal transduction underlying growth cone guidance by diffusible factors. *Curr. Opin. Neurobiol.* **9**, 355-363.
- Varga, Z. M., Amores, A., Lewis, K., Yi-Lin, Y., Postlethwait, J., Eisen, J. and Westerfield, M.** (2001). Zebrafish *smoothened* functions in ventral neuronal tube specification and axon track formation. *Development* **128**, 3497-3509.
- Westerfield, M.** (1995). *The Zebrafish Book*. Eugene, OR: University of Oregon Press.
- Wilson, S. W., Ross, L. S., Parrett, T. and Easter, S. S.** (1990). The development of a simple scaffold of axon tracks in the brain of the embryonic zebrafish, *Branchydanio rerio*. *Development* **108**, 121-145.
- Wilson, S. W. and Easter, S. S., Jr** (1991). Stereotyped pathway selection by growth cones of early epiphyseal neurons in the embryonic zebrafish. *Development* **112**, 723-746.